Coronal and Stellar Mass Ejections
Proceedings IAU Symposium No. 226, 2005
K. P. Dere, J. Wang & Y. Yan, eds.

doi:10.1017/S1743921305000219

Occurrence of Solar Radio Burst Fine Structures in 1–7.6 GHz Range Associated with CME Events

Yihua Yan, Yuying Liu, Zhijun Chen, Qijun Fu, Chengming Tan, Shujuan Wang & Jian Zhang†

National Astronomical Obsevatories, Chinese Academy of Sciences, A20 Datun Road, Chaoyang District, Beijing 100012, China
email: yyh@bao.ac.cn

Abstract. The solar radio bursts and accompanying fine structures recorded by spectrometers at Huairou, Beijing during 1999–2003 are presented. The spectrometers are with high temporal (5–10 ms) and spectral (4–20 MHz) resolutions. We found 91 radio burst events that occurred within half hour of the onset of the CME events which cause solar energetic particle events. The associations of radio fine structures with CME events are discussed.

Keywords. Sun: corona, Sun: coronal mass ejections (CMEs), Sun: Radio

---

1. Introduction

Radio observations at decimetric- and centimeter wavelengths provide important information for inferring fundamental processes of energy release, particle acceleration and particle transport in solar activities (Bastian *et al.* 1998). Temporal fine structures (FS) of solar radio emission in solar flares have been found in various wavebands for several decades (Allaart, *et al.* (1990), Bruggmann, *et al.* (1990), Benz, *et al.* (1992), Sawant, *et al.* (1994), Isliker & Benz (1994), Jiricka, *et al.* (2001), Fu, *et al.* (2004a)). They are considered to be related to primary energy release processes, etc. (Bastian *et al.* 1998). The Solar Radio Broadband Dynamic Spectrometer (SRBS) of China is the first instrument in microwave to acquire dynamic spectrums of solar bursts with the combination of wide frequency coverage (0.7–7.6 GHz), high temporal resolution, high spectral resolution, and high sensitivity (Fu *et al.* 2004b). We compare the occurrence of FSs in 1–7.6 GHz range with flare/CME events.

FSs in >1 GHz range are categoried by Isliker & Benz (1994), Jiricka, *et al.* (2001), Fu, *et al.* (2004a), etc., into different types. Kliem, *et al.* (2000) have found that the radio drifting pulsation structure are associated with CME initial process. Such structure are typical features for the active region NOAA 9077 during its passage over solar disk (Karlicky, *et al.* (2001), Wang, *et al.* (2001a)), and Wang, *et al.* (2001b) found that various radio FSs occurred during different phases for the Bastille Day event. The time sequence of the radio emission was analyzed by comparing with the hard X-rays (HXRs) and the soft X-rays (SXRs) in this flare. After the maxima of the X-rays, the radio emission in the range 1.0–7.6 GHz reached maxima first at the higher frequency, then drifted to the lower frequency. This comparison suggested that the flare included three successive processes: firstly the X-rays rose and reached maxima at 10:10–10:23 UT, accompanied by fine structures only in the lower altitude regime (range 2.6–7.6 GHz); secondly the

† Dept of Astronomy, Beijing University, Beijing, China

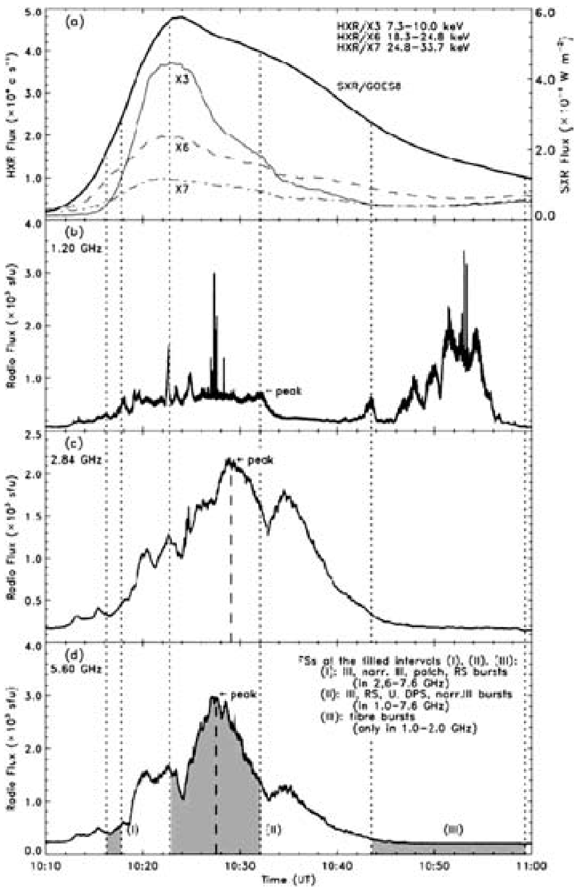

Figure 1. Time profiles of the HXRs and SXR and the radio emission at several typical frequencies during 10:00–11:00 UT on 14 July 2000. (a) HXRs by FY-2 satellite and GOES SXR; (b) 1.2 GHz; (c) 2.84 GHz; and (d) 5.60 GHz. The filled areas in (d) indicate three intervals only in which time interval many radio FSs occurred. During (I) 10:10–10:23 UT, accompanied by fine structures only in the range 2.6–7.6 GHz (II) many fine structures over the range 1.0–7.6 GHz at 10:23–10:34 UT (III) a decimetric type IV burst and its associated FSs (fibers) in the range 1.0–2.0 GHz appeared after 10:40 UT (Wang *et al.* 2001b).

microwave radio emission reached maxima accompanied by many fine structures over the whole altitude (range 1.0–7.6 GHz) at 10:23–10:34 UT; then a decimetric type IV burst and its associated FSs (fibers) in the high altitude regime (range 1.0–2.0 GHz) appeared after 10:40 UT. For the Oct–Nov 2003 flare/CME events, various radio FSs were also found appearing at different phases of the flare/CME process (Tan, *et al.* (2004)).

The temporal relationship between CMEs and associated flares is of great importance to understanding the origin of CMEs. Zhang, *et al.* (2001) have studied this issue using SOHO/LASCO and EIT observations. The association of radio type II bursts and CMEs have been found for decades (Cane (1984), Aurass, (1992)), and Chernov & Markeev (1997) discussed radio FSs in metric wave range associated with CMEs. Here the occurrence of FSs in 1–7.6 GHz with respect to the earth-effective CMEs, that cause solar energetic particle events, is statistically analyzed regardless the FS types. We first introduce the instruments and observations in §2. Then in §3 we present the statistical results and finally we draw our conclusions in §4.

https://doi.org/10.1017/S1743921305000219 Published online by Cambridge University Press

Table 1. The Solar Radio Spectrometers at Huairou/NAOC

Frequency range:	1.0–2.0 GHz	2.6–3.8 GHz	5.2–7.6 GHz
Temporal resolution:	5ms (after June 2002) 20ms (before Dec. 2001)	8ms	5ms
Frequency resolution (MHz/chan.):	4/240 (after June 2002) 20/50 (before Dec. 2001)	10/120	20/120
Sensitivity:	3%,	2%,	2% $S_{\text{quiet Sun}}$
Dynamic range:	10 dB above 3 or 2% $S_{\text{quiet Sun}}$		
Polarizations:	LHCP, RHCP		
Observing time:	22-10UT (Summer), 0-8UT (Winter)		

Table 2. Observed solar radio bursts during 1999–2003 at Huairou/NAOC

Frequency range (GHz):	1.0–2.0	2.6–3.8	5.2–7.6
Number of Burst Events:	729	1616	1198
Number of Fine Structures:	110	131	48

2. Instruments and Observations

Since 1994, a broadband solar radio spectrometer had been developed in China, with a frequency coverage of 0.7–7.6 GHz, a frequency resolution of 1–10 MHz, and a temporal resolution of 1–10 ms (Fu, *et al.* (2004b)). This instrument is composed of multi-bands spectrometers and the three spectrometers at 1.0–2.0 GHz, 2.6–3.8 GHz, and 5.2–7.6 GHz are located at Huairou Solar Observing Station of National Astronomical Observatories, Chinese Academy of Sciences (NAOC). The radio environment has been measured and calibration techniques are developed to ensure reliable observations (Yan, *et al.* (2002), Sych & Yan (2002)).

The performance of the spectrometers is very powerful in detecting radio fine structures. Table 1 shows the description of the spectrometers at Huairou (Ji, *et al.* (2000), Ji, *et al.* (2003), Fu, *et al.* (2004b)).

Many events have been observed since the Chinese Solar Radio Broadband Spectrometers have been put into operation. The radio events observed at Huairou/NAOC during 1999 to 2003 is listed in Table 2.

The radio FSs have also been observed as shown in the above table. Figure 1 shows the occurrence of radio FSs associated with the flare/CME process for the Bastille Day event. For the Oct–Nov 2003 event we also observed FSs during flare/CME process (Tan, *et al.* (2004), Wang, *et al.* (2004)). Here we show the radio zebra pattern and spike fine structures during the rising phase of the 26 October 2003 event in Figure 2.

The CME list is obtained from SOHO/LASCO catalogue (http://cdaw.gsfc.nasa. gov/CME_list/) and the LASCO instrument is introduced in detail by Brueckner, *et al.* (1995).

3. Statistic Results

As mentioned above, we mainly analyze associations of the occurrence of FSs in 1–7.6 GHz with respect to the earth-effective CMEs, i.e., that cause solar energetic particle

https://doi.org/10.1017/S1743921305000219 Published online by Cambridge University Press

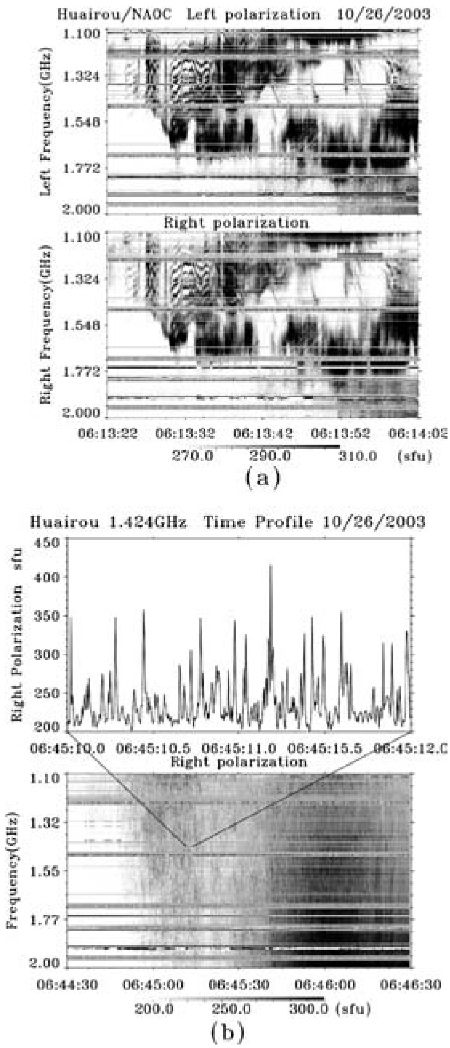

Figure 2. The radio (a) zebra pattern and (b) spike fine structures during the rising phase of the 26 October 2003 event.

events, regardless the FS types. Therefore we chose the radio burst events that occurred within half hour of the onset of the CME events.

During 1997–2003, there were 91 radio burst events in the 1–7.6 GHz range selected which are associated with the CME events, among which 86 were accompanying Type II/IV bursts as shown in Table 3. All these 91 events associated with GOES X-ray flares as listed in Table 3 as well. Among 91 events, 60 (66%) events have burst in all 3 bands employed by Huairou/NAOC spectrometers: 14/18 (78%) for X-class flares 39/57 (68%) for M-class flares and 7/16 (44%) for C-class flares. 78 out of 91 events (85.7%) were associated with Hα flares and the classification is shown in Table 4. If we look at the radio burst events and the GOES X-rays flares we can seen that most of them are radio complex events as shown in Table 5. The importance of the radio flux intensity at 2.84 GHz for these events are listed in Table 6. It can be seen that most are strong radio burst

Table 3. Radio bursts (in 1–7.6 GHz) associated with CMEs and Type II/IV bursts and SXR flares

CMEs	Type II	Type IV	X	M	C
91 (100%)	49 (54%)	37 (41%)	18 (20%)	57 (62%)	16 (18%)

Table 4. Radio bursts (in 1–7.6 GHz) associated with CMEs and Hα flares

Total event	3B	2B	1B	SF	1N	others	no flare
91	4	17	7	13	17	20	13

Table 5. Classification of soft X-ray flares

GOES flare	Event	47GB	45 C	5 S	3 S	1 S	Other
X class	18	16	1	1	0	0	0
M class	57	15	27	4	9	1	1
C class	16	0	6	6	4	0	0
Total	91	31	34	11	13	1	1

events. This is agreeable to the selection that the CME events are all earth-directed and caused SEP events.

In all 91 events there are 38 (41.7%) containing FSs (or FS groups). The 26 FSs occurred during rising phase, 16 during maximum, and 8 in decaying phase (there are overlaps for FS occurrence). Note here a FS event may contain different types of FSs as we mentioned above. The detailed description of these events are listed in Table 7. We have also analyzed the time sequences of these flare/CME event and the results are listed in Table 8. It can be seen that most events are in radio burst-SXR flare maximum-CME time sequences. Please note that radio bursts and flares are measured at their peak time whereas the CME onsets are measured according to their C2/C3 onset time. Therefore it deserves careful analysis of these time sequence relationship.

4. Conclusions

In summary, during 1997–2003, there were 91 radio burst events in the 1−7.6 GHz range selected which are associated with the CME events that caused SEP events. The CME was simply chosen when they are half hour apart to the radio bursts and SXR flares.

(1) All the events are associated with soft X-ray flares (18 X class, 57 M class and 16 C class events), 78 are associated with Hα flares, 49 associated with Type II burst and 37 with Type IV burst.

(2) In the 91 CME-associated radio burst events, 60 (66%) have burst in all 3 frequency bands: 14/18 (78%) for X-class 39/57 (68%) for M-class and 7/16 (44%) for C-class. Most of them are of complex radio burst profiles (65 events) and with strong intensity (71 events with >100 s.f.u. at 2.84 GHz). 50 events (65%) were in a time sequence of "radio burst" → "SXR flare" → "CME onset".

(3) There are 38 (41.7%) event containing FSs (or FS groups). Most radio FSs occurred during rising phase of flare/CMEs, and the occurrence of FSs decreases as frequency

https://doi.org/10.1017/S1743921305000219 Published online by Cambridge University Press

Table 6. Solar Radio Flux at 2.84 GHz of the events

Flux range (s.f.u.)	< 100	$100 - 500$	$500 - 1000$	$1000 - 5000$	> 5000
Events	20	40	14	16	1

Table 7. Occurrence of radio FSs in different burst phases

Phases:	rising	peak	decay
1–2 GHz	19	15	4
2.6–3.8 GHz	14	3	3
5.2–7.6 GHz	5	2	1

Table 8. Time sequences of radio burst/CME/falres.

Radio burst maximum → SXR flare maximum → CME	59	(65%)
Radio burst maximum → CME → SXR flare maximum	8	(9%)
SXR flare maximum → Radio burst maximum → CME	12	(13%)
SXR flare maximum → CME → Radio burst maximum	2	(2%)
CME → Radio burst maximum → SXR flare maximum	7	(8%)
CME → SXR flare maximum → Radio burst maximum	3	(3%)

increases (19/14/5 FS events in rising, 15/3/2 at peak, and 4/3/1 when decay for 1–2 G/2.6–3.8 G/5.2–7.6 GHz regime).

(4) If we consider a standard flare/CME model the above statistic results are consistent with such a scenario and radio fine structures may manifest initial phase signature, which is important to diagnose coronal parameters.

Acknowledgements

The work is supported by CAS, NSFC grants 10225313, 10333030, and MOST grant G2000078403. We acknowledge SOHO/LASCO for providing CME catalog used in this study.

References

Allaart, M. A. F., van Nieuwkoop, J., Slottje, C., & Sondaar, L. H. 1990, *Sol. Phys.* 130, 183
Aurass, H. 1992, *Ann. Geophys.* 10, 359
Bastian, T. S., Benz, A. O., & Gary, D. E. 1998, *ARAA* 36, 131
Benz, A. O., Su, H., Magun, A., & Stehling, W. 1992, *A&A* 93, 539
Brueckner, G. E., Howard, R. A., Koomen, M. J., & *et al.* 1995, *Sol. Phys.* 162, 357
Bruggmann, G., Magun, A., Benz, A. O., & Stehling, W. 1990, *A&ASS* 240, 506
Cane, H. V. 1984, *A&A* 140, 205
Chernov, G. P., & Markeev, A. K. 1997, *IAU JD* 19, 16
Fu, Q., Yan, Y., Liu, Y., & *et al.* 2004a, *Chin. J. Astron. Astrophys.* 4, 176
Fu, Q., Ji, H., Qin, Z., & *et al.* 2004b, *Sol. Phys.* 222, 167
Isliker, II., & Benz, A. 1994, *A&A* 105, 205
Ji, II., Fu, Q., Liu, Y., & *et al.* 2000, *ACTA Astrophysica Sinica* 20, 209
Ji, H., Fu, Q., Liu, Y., & *et al.* 2003, *Sol. Phys.* 213, 359
Jiricka, T., & *et al.* 2001, *A&A* 375, 243
Karlicky, M., Yan, Y. H., Fu, Q. J., & *et al.* 2001, *A&A* 369, 1104
Kliem, B., Karlicky, M., & Benz, A. O. 2000, *A&A* 360, 715
Sawant, H. S., Fernandes, F. C. R., & Neri, J. A. C. F. 1994, *ApJS* 90, 689

Sych, R. A., & Yan, Y. H. 2002, Chin. J. Astron. Astrophys. 2, 183
Tan, C.-M., Fu, Q.-j., Yan, Y.-H., & Liu, Y-Y. 2004, *Chin. J. Astron. Astrophys.* 4, 205
Wang, S. J., Yan, Y. H., & Fu, Q. J. 2001a, *A&A* 370, L13
Wang, S. J., Yan, Y. II., Zhao, R. Z., & *et al.* 2001b, *Sol. Phys.* 204, 153
Wang, S. J., & *et al.* 2004, *IAU Symp* 226 (these proceedings)
Yan, Y., Tan, C., Xu, L., Ji, H., Fu, Q., & Song, G. 2002, *Since in China (Series A)* 45, 89
Zhang, J., Dere, K. P., Howard, R. A., Kundu, M. R., & White, S. M. 2001, *ApJ* 559, 452

https://doi.org/10.1017/S1743921305000219 Published online by Cambridge University Press